PERGAMON

International Journal of Heat and Mass Transfer 43 (2000) 2089–2099

International Journal of HEAT and MASS TRANSFER

www.elsevier.com/locate/ijhmt

Entropy generation for natural convection in an inclined porous cavity

A.C. Baytaş

Istanbul Technical University, Institute for Nuclear Energy, 80626 — Maslak, Istanbul, Turkey

Received 30 March 1999; received in revised form 16 September 1999

Abstract

The issue of entropy generation in a tilted saturated porous cavity for laminar natural convection heat transfer is analysed by solving numerically the mass, momentum and energy balance equations, using Darcy's law and Boussinesq-incompressible approximation. As boundary conditions of cavity, two opposite walls are kept at constant but different temperatures and the other two are thermally insulated. The parameters considered are the angle of inclination and the Darcy–Rayleigh number. When available, present solutions are compared with known results from the previous researches. Excellent agreement was obtained between results that validate the used computer code. The results show that the calculation of local entropy generation maps are feasible and can supply useful information for the selection of a suitable angle of inclination.

Keywords: Entropy generation; Porous media; Natural convection; Cavity

1. Introduction

In computational simulation of thermal-hydraulic unsteady investigations, the quantities to be calculated are usually temperature, velocity fields, enthalpy, pressure, etc.; but rarely contains entropy properties using the second law of thermodynamics. Principally, only heat transfer was reflected in natural convection studies. The necessity for the utilisation of the second law of thermodynamics in thermal design decisions is vividly demonstrated in this research work. The research of natural convection in porous media has been conducted widely in recent years, which involves post-accidental heat removal in nuclear reactors, cooling of radioactive waste containers, heat exchangers, solar power collectors, grain storage, food processing, energy efficient drying processes, to name of a few. Nield and Bejan [1] and Ingham and Pop [2] contributed to a wide overview of this important area in heat transfer of porous media. There are many published studies related to natural convection in rectangular porous enclosures. Moya et al. [3], Bejan [4], Parasad and Kulacki [5], Baytas and Pop [6], Beckerman et al. [7], Gross et al. [8], Lai and Kulacki [9], Monale and Lage [10], and Walker and Homsy [11] have donated many important results for this problem. Caltagirone and Bories [12] studied the stability criteria of free convective flow in an inclined porous layer. Moya et al. [3] investigated the natural convection problem for tilted rectangular porous material and in other contributions by Vasseur et al. [13] and Sen et al. [14]. The literature on the natural convection of inclined porous enclosure is limited. Besides, only a very small number of studies were published in the past years considering the entropy generation in convective heat transfer of enclosure problems.

E-mail address: baytas@itu.edu.tr (A.C. Baytaş).

0017-9310/00/$ - see front matter
PII: S0017-9310(99)00291-4

Nomenclature

Be	Bejan number, Eq. (12)
FFI	Fluid Friction Irreversibility, Eq. (9)
g	acceleration due to gravity (m/s^2)
HTI	Heat Transfer Irreversibility, Eq. (9)
k	effective thermal conductivity of the porous medium (W/m K)
K	permeability of the porous medium (m^2)
L	cavity length (m)
N	local entropy generation, Eq. (9)
N_S	entropy generation number, Eq. (11)
Nu	local Nusselt number, Eq. (6)
Nu_a	average Nusselt number, Eq. (7)
Ra	Rayleigh number, Eq. (4)
S_{gen}^{m}	entropy generation rate per unit volume (W/m^3 K)
t	time (s)
T	fluid temperature (K)
T_C	temperature of the cold wall (K)
T_H	temperature of the hot wall (K)
T_0	-$(T_H + T_C)/2$ (K)
ΔT	temperature difference, $\Delta T = T_H - T_C$ (K)
u, v	velocity components in x, y directions (m/s)
U, V	dimensionless velocity components in X, Y directions
x, y	Cartesian coordinates (m)
X, Y	dimensionless coordinates

Greek symbols

α	effective thermal diffusivity of the porous medium (m^2/s)
β	coefficient of thermal expansion (K^{-1})
Θ	dimensionless temperature, Eq. (4)
μ	dynamic viscosity (kg/m s)
ν	kinematic viscosity (m^2/s)
σ	ratio of heat capacity of porous medium to that of fluid
φ	inclined angle (deg), Fig. 1
τ	dimensionless time, Eq. (4)
ϕ	irreversibility distribution ratio, Eq. (10)
ψ	stream function (m^2/s)
Ψ	dimensionless stream function, Eq. (4)

The utilisation of the second law of thermodynamics in convective heat transfer is very well presented in Refs. [15–19]. Drost and White [20] studied numerical calculation of local entropy generation map in an impinging jet. San et al. [21] studied entropy generation in convective heat and mass transfer within a smooth channel under some specific thermal boundary conditions. Cheng et al. [22] presented a numerical study of entropy generation for mixed convection in a vertical channel with transverse fin array. Baytas [23] studied the optimisation in an inclined enclosure for minimum entropy generation in natural convection for the first time.

This presented that the main subject of the investigation is not only computational heat transfer of porous cavity but also to investigate entropy generation distribution according to inclination angle for saturated porous cavity by using the second law of thermodynamics. The present paper reports a numerical entropy generation calculations of the two-dimensional laminar free convection flow in an inclined cavity filled with a saturated porous medium. The effect of the inclination angle (φ) on the flow and heat transfer characteristics and the entropy generation was studied by varying φ from 0° to 360° and dimensionless *Ra* from 10^2 to 10^4. The isotherms, the patterns of streamlines and their corresponding entropy generation maps, the variation of entropy generation due to heat transfer and fluid friction irreversibility versus inclination angle for different Rayleigh numbers are presented in graphical forms. A numerical study about the entropy generation for natural convection in an inclined porous cavity by using the second law of thermodynamics has not yet been encountered.

2. Mathematical modelling

Consider the flow of a Newtonian fluid within a square porous enclosure as depicted in Fig. 1. The non-dimensional governing equations are obtained with following assumptions; in porous cavity, Darcy's law is assumed to hold, the fluid is assumed to be a normal

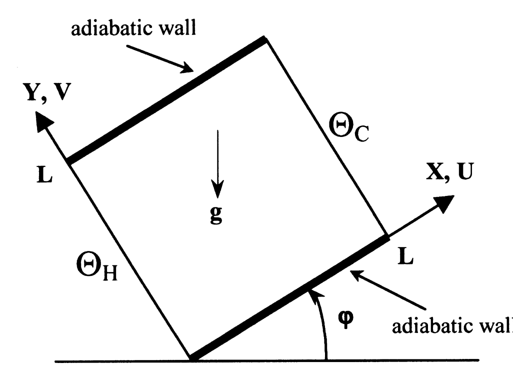

Fig. 1. Physical model of the 2D inclined porous cavity.

Boussinesq-incompressible fluid and inertial effects are neglected. The saturated porous medium is assumed to be isotropic in thermal conductivity. Finally, the set of non-dimensional governing equations in terms of the stream function Ψ and temperature Θ are

$$\frac{\partial^2\Psi}{\partial X^2}+\frac{\partial^2\Psi}{\partial Y^2}=Ra\left(\cos\varphi\frac{\partial\Theta}{\partial X}-\sin\varphi\frac{\partial\Theta}{\partial Y}\right) \tag{1}$$

and

$$\frac{\partial\Theta}{\partial\tau}+U\frac{\partial\Theta}{\partial X}+V\frac{\partial\Theta}{\partial Y}=\frac{\partial^2\Theta}{\partial X^2}+\frac{\partial^2\Theta}{\partial Y^2} \tag{2}$$

The velocity equations:

$$U=\frac{\partial\Psi}{\partial Y};\qquad V=-\frac{\partial\Psi}{\partial X} \tag{3}$$

where the non-dimensional variables are defined by

$$X,\ Y=x,\ y/L;\quad \Psi=\psi/\alpha;\quad U,\ V=u,\ v/(\alpha/L)$$

$$\tau=t\left(\frac{\alpha}{\sigma L^2}\right);\quad Ra=\frac{gK\beta\Delta TL}{\alpha\nu};\quad \Theta=\frac{T-T_0}{T_H-T_C} \tag{4}$$

Eqs. (1) and (2) are subjected to following initial and boundary conditions:

$\tau\le 0$ for whole space:

$$\Theta=\Psi=0$$

$\tau>0$:

$$\psi=0,\ \Theta=0.5 \text{ on plane } X=0$$

$$\psi=0,\ \Theta=-0.5 \text{ on plane } X=1$$

$$\psi=0,\ \frac{\partial\Theta}{\partial Y}=0 \text{ on } Y=0,\ 1 \tag{5}$$

The local Nusselt number is defined as

$$Nu=\frac{\partial\Theta}{\partial Y}|_{X=0,\ 1} \tag{6}$$

And the average Nusselt number is

$$Nu_a=\int_0^1 Nu\,\mathrm{d}Y \tag{7}$$

3. Entropy generation due to convection heat transfer

The non-equilibrium conditions due to the exchange of energy and momentum, within the fluid and at the solid boundaries, cause a continuous entropy generation in the flow field of porous cavity. This entropy generation is due to the irreversible nature of heat transfer and viscosity effects, within the fluid and at the solid boundaries. From the known temperature and velocity fields, volumetric entropy generation can be calculated by the equation [17],

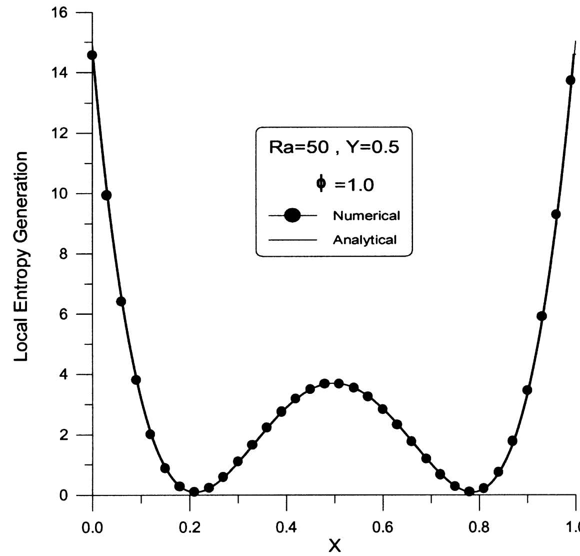

Fig. 2. Benchmarking of the predicted local entropy generation with analytical solution.

$$S_{\text{gen}}^{\text{m}}=\frac{k}{T_0^2}(\nabla T)^2+\frac{\mu}{KT_0}\left(U^2+V^2\right) \tag{8}$$

Dimensionless form of Eq. (8) can be obtained by utilising the dimensionless variable listed in Eq. (4) and then defining the local entropy generation number, N, for 2D square cavity of Fig. 1 as given below

$$N=\underbrace{(\nabla\Theta)^2}_{\text{HTI}}+\underbrace{\phi(\nabla\Psi)^2}_{\text{FFI}} \tag{9}$$

where ϕ is the irreversibility distribution ratio

$$\phi=\frac{\mu T_0}{k}\left[\frac{\alpha^2}{K(\Delta T)^2}\right] \tag{10}$$

The local entropy generation number would be integrated over the whole domain to obtain the entropy generation number for whole cavity volume as

$$N_S=\int_0^1\int_0^1 N\,\mathrm{d}X\,\mathrm{d}Y \tag{11}$$

In this study, the dimensionless Bejan number (Be) [16] is used as the alternative irreversibility distribution

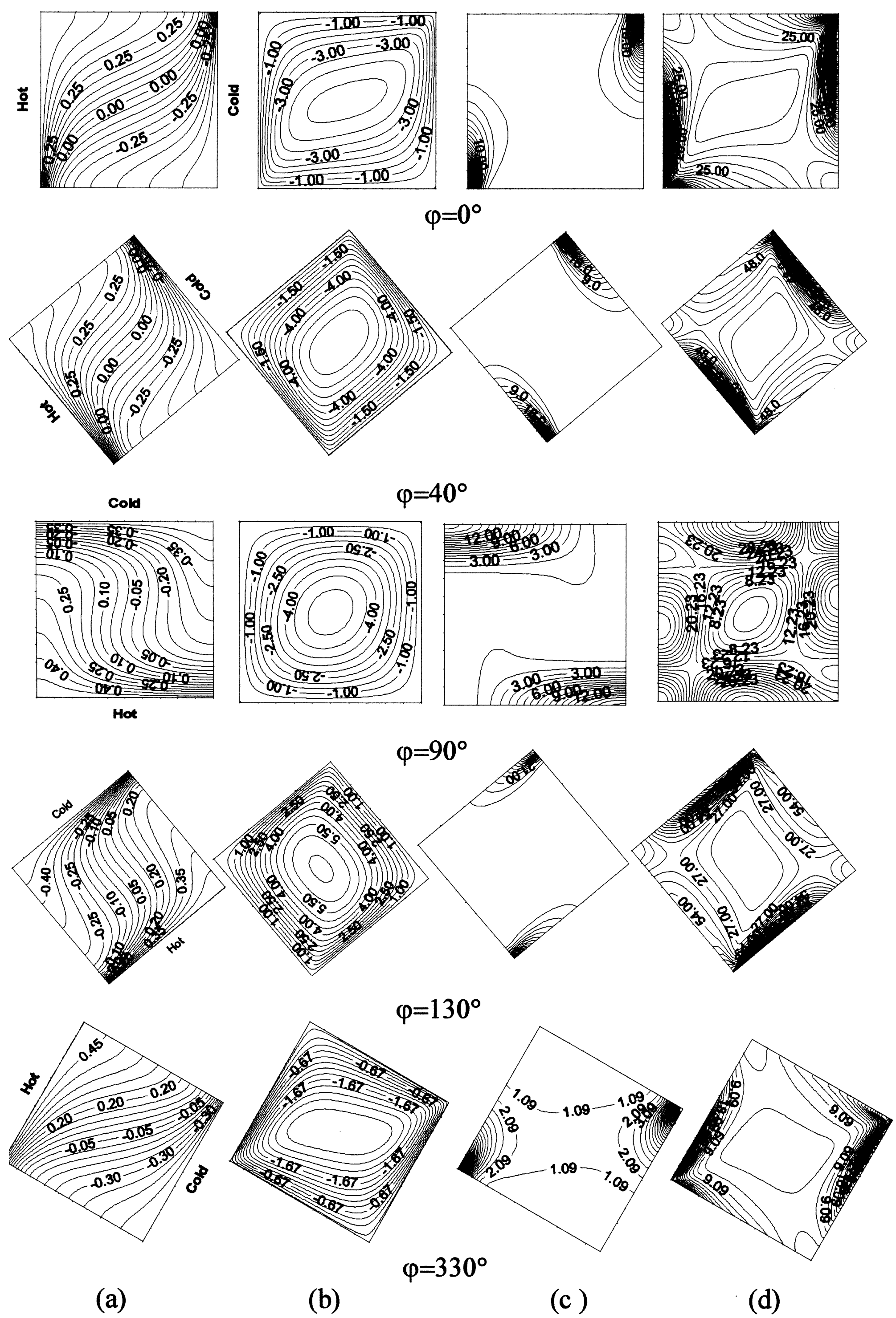

Fig. 3. (a) Isotherms, (b) streamlines, (c) entropy generation due to heat transfer and (d) the local entropy generation (N) at different inclined angles for $Ra = 10^2$.

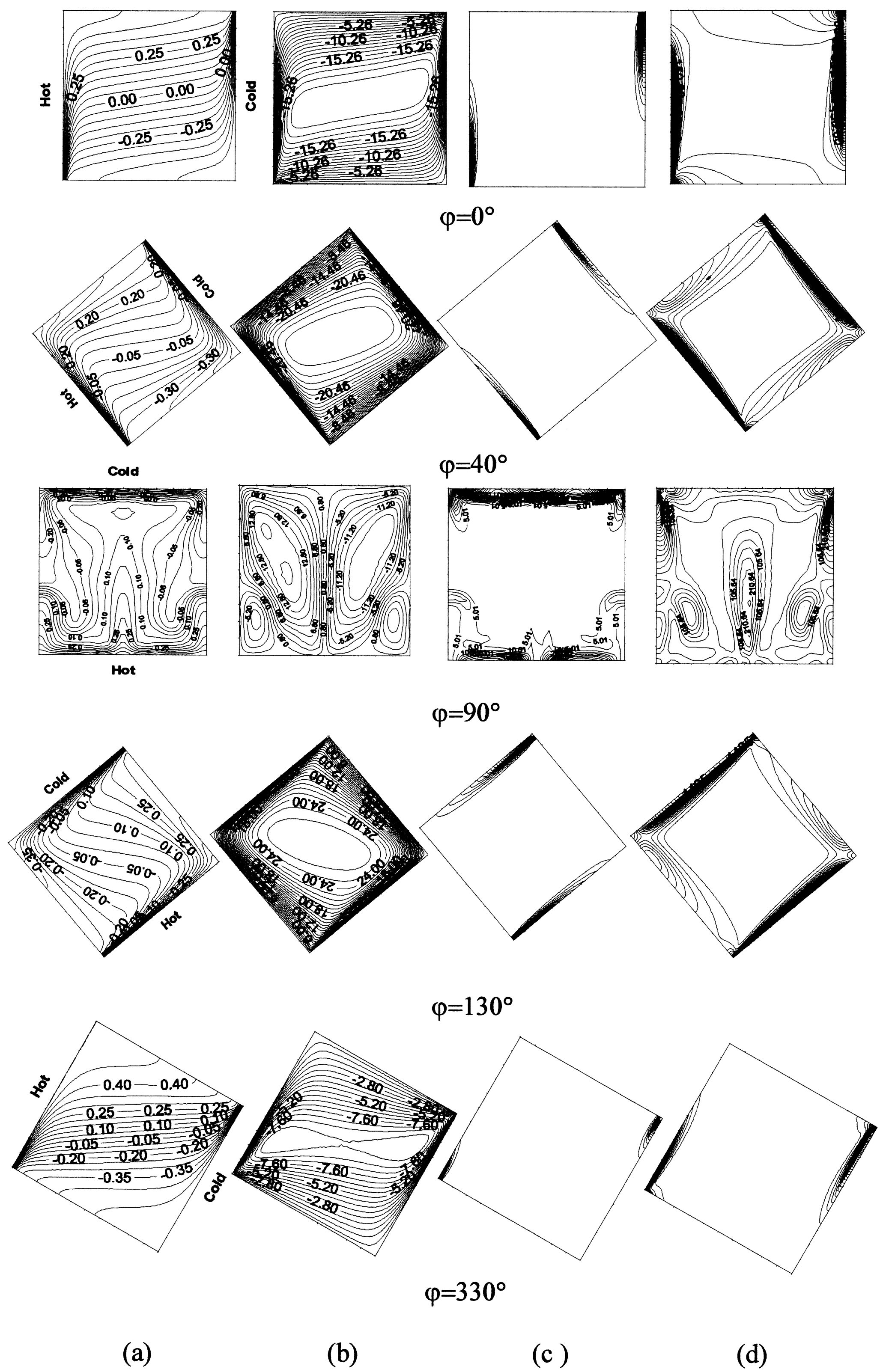

Fig. 4. (a) Isotherms, (b) streamlines, (c) entropy generation due to heat transfer and (d) the local entropy generation (N) at different inclined angles for $Ra = 10^3$.

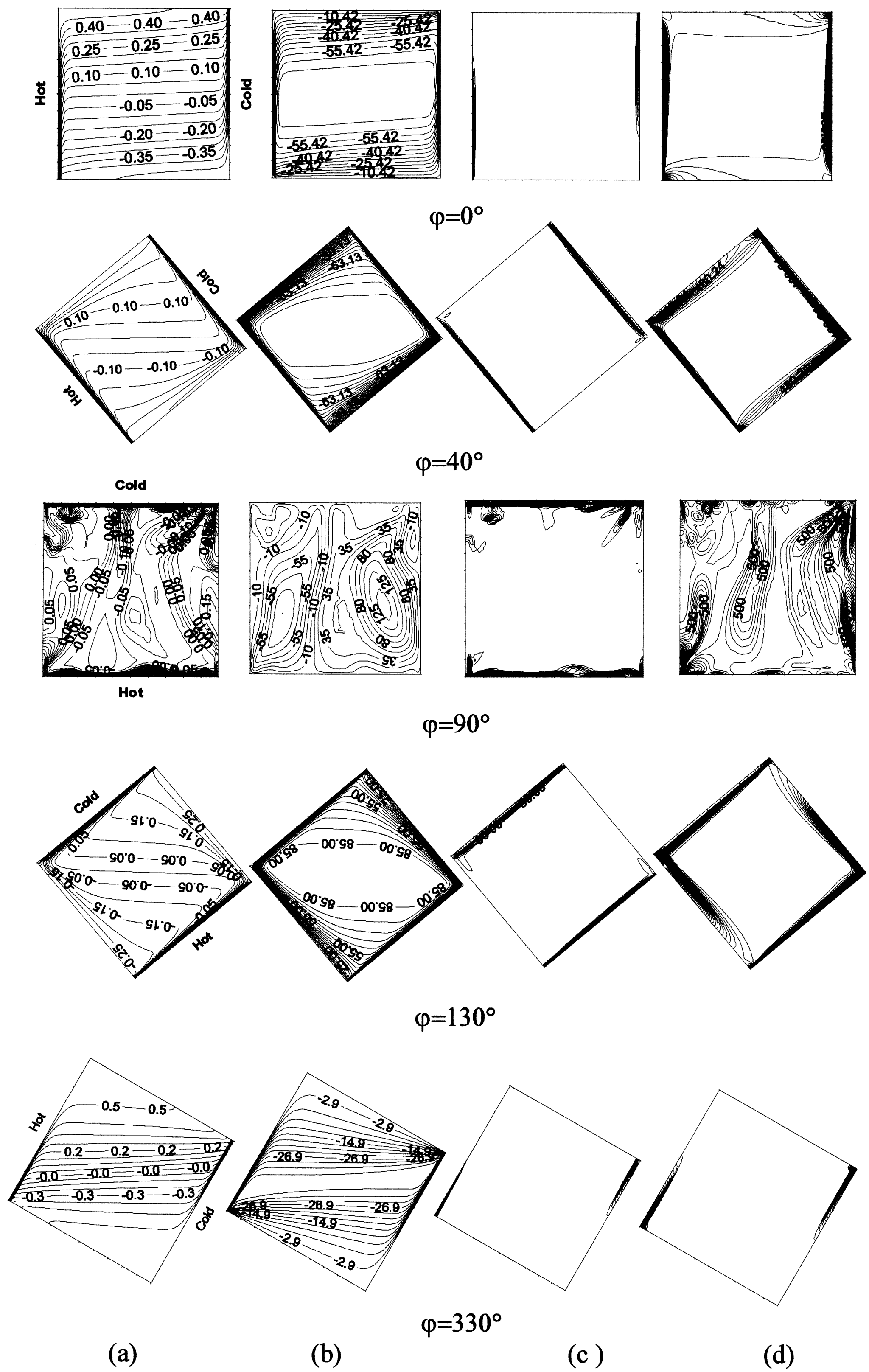

Fig. 5. (a) Isotherms, (b) streamlines, (c) entropy generation due to heat transfer and (d) the local entropy generation (N) at different inclined angles for for $Ra = 10^4$.

number for inclined porous cavity from Eq. (9), as follows:

$$Be = \frac{(\nabla\Theta)^2}{(\nabla\Theta)^2 + (\nabla\Psi)^2} \tag{12}$$

4. Benchmark solution for entropy generation

For benchmarking purpose, the analytical solution for temperature and stream function given in Ref. [24], Eqs. (18) and (20), was used for natural convection in a porous enclosure. From these analytical solutions, local entropy generation map and entropy generation number were calculated by utilising MATHEMATICA version 3.0. These results of MATHEMATICA were compared with numerical results from the developed computer program. This comparison (for Eq. (9)) is shown in Fig. 2 for $Y = 0.5$ and $Ra = 50$. It is clear from Fig. 2 that the numerical and analytical results are best matched. Benchmark results from Eq. (11) for $Ra = 50$ by MATHEMATICA and developed computer code are 2.48829 and 2.4880078, respectively.

5. Result and discussion

The governing equations (1)–(3) were solved numerically using Finite Difference Control Volume Method of Patankar [25] along with boundary conditions given in Eq. (5). Resulting algebraic equations were solved by Alternating Direction Implicit (ADI) method. The numerical details of solution method are given in Ref. [23,26,27]. The presented numerical study was checked for accuracy against the earlier published numerical results reported by different authors, and the agreement between the present and previous results was very good in Ref. [6]. For this reason, it is not repeated here for brevity.

This investigation is mainly concerned about entropy generation distribution within an inclined porous square cavity by using the second law of thermodynamics. Results are presented for inclination angle, φ (in Fig. 1) from 0° to 360° and Rayleigh number from

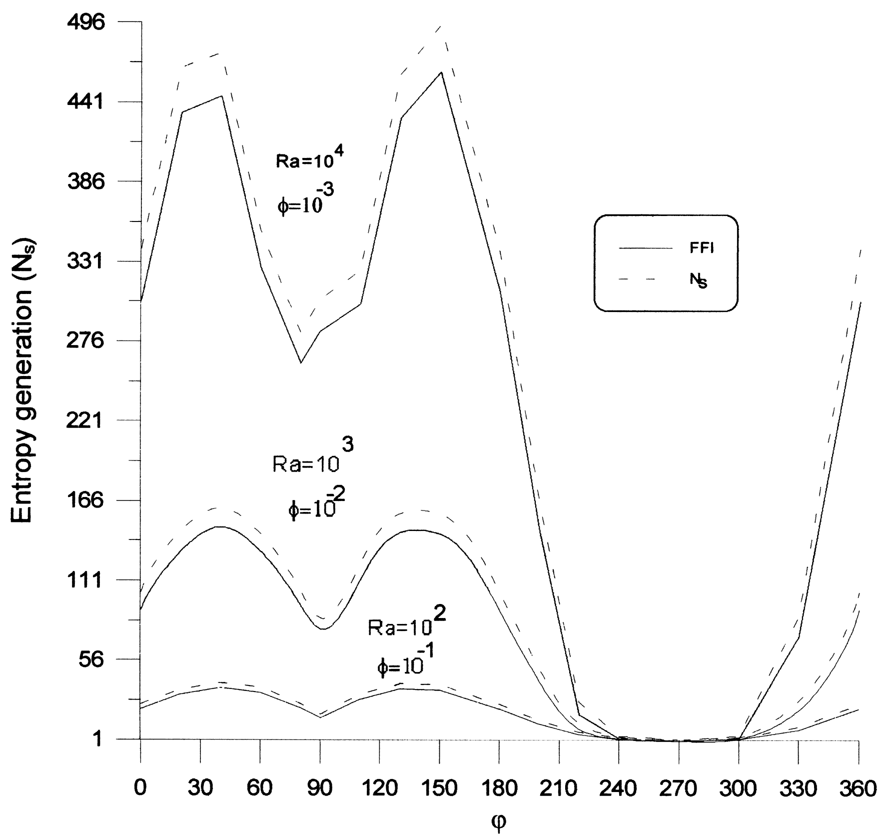

Fig. 6. Variation of entropy generation number (N_S) and FFI versus inclined angle.

10^2 to 10^4. Benchmark solution for this analysis is given in Ref. [6]. It was concluded that the present results match very well with previously published results. In Figs. 3–5, isotherms, streamlines, entropy generation due to heat transfer and local entropy generation number (Eq. (9)) are shown graphically for $Ra = 10^2$, 10^3 and 10^4, respectively. In Fig. 3(c) for $\varphi = 0°$, it is clear that entropy generation is higher at high temperature gradients (Fig. 3(a)). This is due to heat transfer irreversibility because large heat transfer is confined to these locations. As is clear from Fig. 3(c) for $\varphi = 0°$, entropy generation is mainly confined to the lower and upper corners for the left and right walls, respectively. This entropy generation length along the wall increases for $\varphi = 40°$ and 90° for the same Ra (Fig. 3(c)). After $\varphi = 90°$, the entropy generation length along the wall reduces gradually for $\varphi =$ 130° and 330°. It is evident that entropy generation is directly proportional to temperature gradients. Above discussion is equally valid for Figs. 4(c) and 5(c). For $Ra = 10^3$ in Fig. 4(c), the entropy generation covers the whole heated and cooled walls for $\varphi = 90°$; while for $Ra = 10^4$ (Fig. 5(c)), this is true for $\varphi = 40°$, 90° and 130°.

Distribution of local entropy generation due to heat transfer and fluid flow, collectively, is shown in Figs. 3–5(d). As is clear from Fig. 3(d), entropy generation covers almost whole domain for $Ra = 10^2$, while this covered part of the domain reduces as the Rayleigh number increases (Figs. 4 and 5). In case of $Ra = 10^4$, the entropy generation is localised along the walls only (Fig. 5(d)). It is evident from the above-mentioned figures that most of the domain is not involved in entropy generation for higher Ra, excluding the case for $\varphi = 90°$. This is due to the boundary layer regime at high Rayleigh numbers.

Variation of fluid friction irreversibility (FFI) and entropy generation number (N_S), for different angular positions, are shown in Fig. 6. Flow is converted into conduction regime for all the Rayleigh numbers from 240° to 300°. This is due to the reason that buoyancy is no longer available between these angles. FFI and N_S show a repetition of behaviour from 0° to 90° and from 90° to 200°. As shown in Fig. 6, FFI has a minimum at 90° for $Ra = 10^2$ and 10^3, whereas FFI has a minimum at 80° for $Ra = 10^4$. As is expected, the values of FFI and N_S increase with increasing Rayleigh number. Nu_a and HTI are plotted in Fig. 7 against the

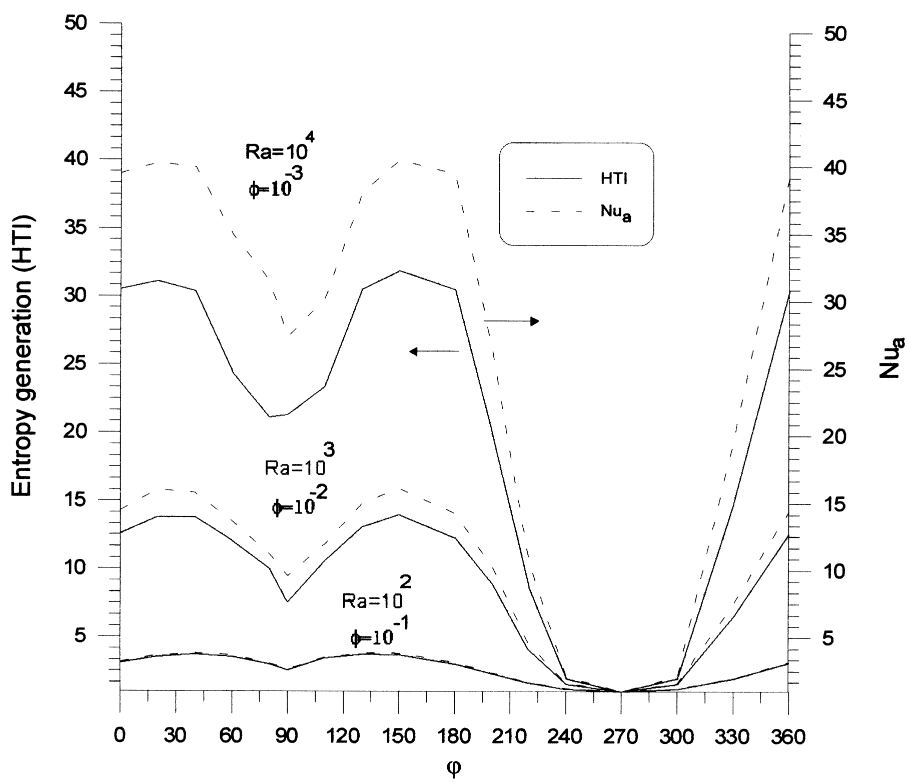

Fig. 7. Variation of entropy generation due to heat transfer (HTI) and average Nusselt number versus inclined angle.

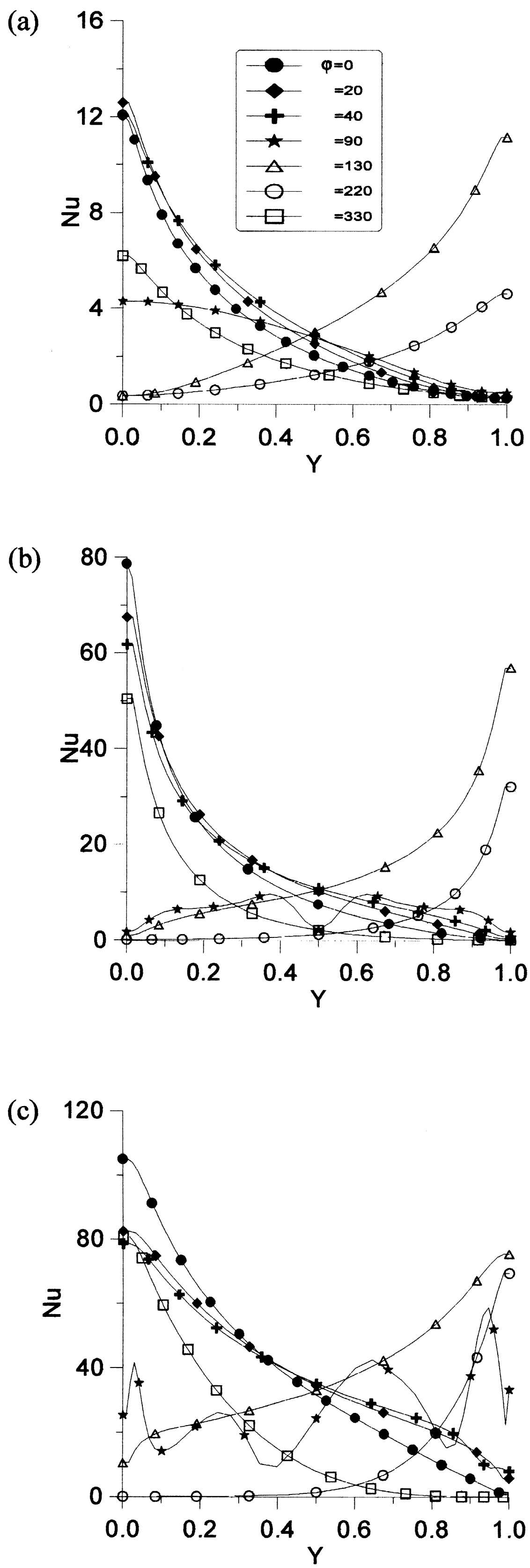

angular location (φ). Again their overall behaviour is almost similar to that of FFI and N_S in Fig. 6, and also HTI has a minimum at 80° for $Ra = 10^4$, while it has a minimum at 90° for $Ra = 10^2$ and 10^3.

In Fig. 8, the local Nusselt number variation is shown graphically for hot wall. In case of angular positions of 0°, 20°, 40° and 330°, the local Nusselt number is highest at the bottom of the cavity while it is lowest at the top. However, the trend is reversed when $\varphi = 130°$ and 220°. This is due to reversal of buoyancy effect. There is a remarkable difference for $\varphi = 90°$ from all other values of φ for $Ra = 10^3$ and 10^4.

In Fig. 9, the variation of Bejan number (Be) versus inclination angle (φ) is shown as an alternative irreversibility distribution parameter as described in Eq. (12). As defined in Ref. [16], $Be = 1.0$ is the limit at which all the irreversibility is due to heat transfer, $Be = 0$ is the opposite limit at which all the irreversibility is due to fluid friction, and $Be = 1/2$ is the case in which the heat transfer and fluid friction entropy generation rates are equal. $Be \gg 1/2$ is the case where the irreversibility due to heat transfer dominates, while $Be \ll 1/2$ is the case where the irreversibility due to fluid friction dominates. As seen in Fig. 9, $Be = 1.0$ at $\varphi = 270°$ is the limit at which the heat transfer irreversibility dominates. As Rayleigh number decreases, heat transfer irreversibility is dominant around $\varphi = 270°$. For high Rayleigh number, fluid friction irreversibility dominates for porous cavity except around $\varphi = 270°$ as is clear from Fig. 9. As shown in Fig. 9, Bejan number changes more rapidly when Ra and φ increase after inclined angle $\varphi = 180°$.

The Bejan number is clearly a measure of the relative magnitude of the heat transfer and fluid friction irreversibilities. The Bejan number has small values for the inclination angles between 30° to 60° and 120° to 170° in Fig. 9. It shows that the heat transfer and fluid friction contribution to the irreversible losses are not comparable in these flow cases. It shows evidently that in these inclination angles, convective heat transfer is dominated as seen Nu_a in Fig. 7 and also fluid friction irreversibility is dominated.

6. Conclusions

The distribution of entropy generation in 2D laminar natural convective flows for saturated tilted porous cavity has been studied numerically by using ADI,

Fig. 8. Local Nusselt number along the hot wall for various inclined angle; (a) $Ra = 10^2$, (b) $Ra = 10^3$ and (c) $Ra = 10^4$.

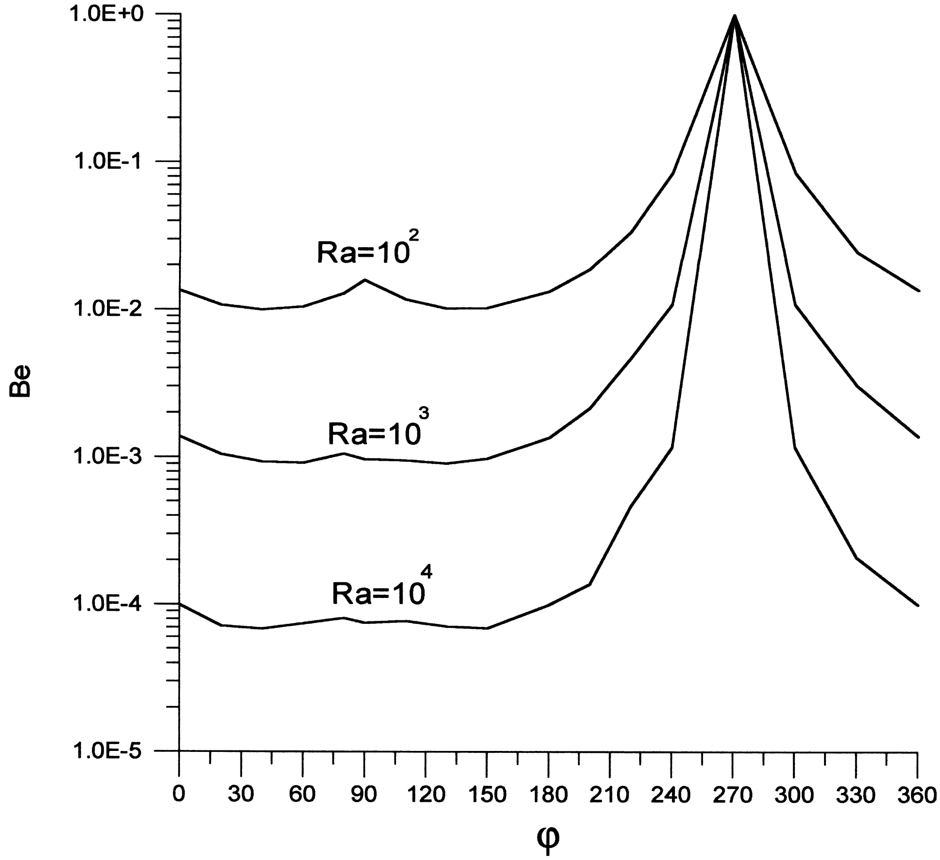

Fig. 9. Variation of Bejan number (Be) with inclined angle for $Ra = 10^2$, 10^3 and 10^4.

Finite Difference Method and the Second Law of Thermodynamics. The present solutions for a porous cavity are compared with the known results from open literature. It was found that these results are in very good agreement. A new computer program was developed to compute the distribution of entropy generation for present problem. The comparison of numerical and analytical results for a simple benchmarking problem of entropy generation was successful. The influences of the physical parameters, Ra, Be, and φ are evaluated. Results show that when Ra decreases, heat transfer irreversibility begins to dominate the fluid friction irreversibility. The Bejan number is rapidly changed between 150° and 270°.

The entropy generation contains two physical levels: at a local level in Figs. 3–5, it shows not only where irreversibilities are present, but also to what extent they are sensitive to design changes according to different inclination angle; at a integral level in Figs. 6, 7 and 9, it gives a measure of the "degree of irreversibility" of the convective flow in the enclosure.

Acknowledgements

This paper has been supported by the ITU Research Fund, through grant 843.

References

[1] D.A. Nield, A. Bejan, Convection in Porous Media, Springer, New York, 1998.

[2] D.B. Ingham, I. Pop (Eds.), Transport Phenomena in Porous Media, Elsevier, Amsterdam, 1998.

[3] S.L. Moya, E. Ramos, M. Sen, Numerical study of natural convection in a tilted rectangular porous material., Int. J. Heat Mass Transfer 30 (1987) 741–756.

[4] A. Bejan, On the boundary layer regime in a vertical enclosure filled with a porous medium, Lett. Heat Mass Transfer 6 (1979) 93–102.

[5] V. Prasad, F.A. Kulacki, Convective heat transfer in a rectangular porous cavity effect of aspect ratio on flow structure and heat transfer, J. Heat Transfer 106 (1984) 158–165.

[6] A.C. Baytas, I. Pop, Free convection in oblique enclosures filled with a porous medium, Int. J. Heat Mass transfer 42 (1999) 1047–1057.

[7] C. Beckermann, R. Viskanta, S. Ramadhyani, A numerical study of non-Darcian natural convection in a vertical enclosure filled with a porous medium, Num. Heat Transfer 10 (1986) 557–570.

[8] R.J. Gross, M.R. Bear, C.E. Hickox, The application of flux-corrected transport (FCT) to high Rayleigh number natural convection in a porous medium, in: Proc. 8th Int. Heat Transfer Conf., San Francisco, CA, 1986.

[9] F.C. Lai, F.A. Kulacki, Natural convection across a vertical layered porous cavity, Int. J. Heat Mass Transfer 31 (1988) 1247–1260.

[10] D.M. Manole, J.L. Lage, Numerical Benchmark results for natural convection in a porous medium cavity, in: ASME Conference, Heat and Mass Transfer in Porous Media, HTD-Vol. 216, 1992, 55–60.

[11] K.L. Walker, G.M. Homsy, Convection in a porous cavity, J. Fluid Mech 87 (1978) 449–474.

[12] J.-P. Caltagirone, S. Bories, Solutions and stability criteria of natural convective flow in an inclined porous layer, J. Fluid Mech. 155 (1985) 267–287.

[13] P. Vasseur, M.G. Satish, L. Robillard, Natural convection in a thin inclined porous layer exposed to a constant heat flux, Int. J. Heat Mass Transfer 30 (1987) 537–549.

[14] M. Sen, P. Vasseur, L. Robillard, Multiple steady states for unicellular natural convection in an inclined porous layer, Int. J. Heat Mass Transfer 30 (1987) 2097–2113.

[15] A. Bejan, Entropy Generation Through Heat and Fluid Flow, 2nd ed., Wiley, New York, 1994.

[16] A. Bejan, Entropy Generation Minimisation, CRC Press, Boca Raton, FL, 1996.

[17] A. Bejan, Convection Heat Transfer, 2nd ed., Wiley, New York, 1995.

[18] A. Bejan, A study of entropy generation in fundamental convective heat transfer, J. of Heat Transfer 110 (1979) 718–725.

[19] D. Poulikakos, A. Bejan, Fin geometry for minimum entropy generation in forced convection, J. of Heat Transfer 104 (1982) 616–623.

[20] M.K. Drost, M.D. White, Numerical predictions of local entropy generation in an impinging jet, J. of Heat Transfer 113 (1991) 823–829.

[21] J.Y. San, W.M. Worek, Z. Lavan, Entropy generation in convective heat transfer and isothermal convective mass transfer, J. of Heat Transfer 109 (1987) 647–652.

[22] C.H. Cheng, W.P. Ma, W.H. Huang, Numerical predictions of entropy generation for mixed convective flows in a vertical channel with transverse fin arrays, Int. J. Heat Mass Transfer 21 (1994) 519–530.

[23] A.C. Baytas, Optimisation in an inclined enclosure for minimum entropy generation in natural convection, J. Non-Equil. Thermodyn 22 (1997) 145–155.

[24] M. Haajizadeh, A.F. Ozguc, C.L. Tien, Natural convection in a vertical porous enclosure with internal heat generation, Int. J. Heat Mass Transfer 27 (1984) 1893–1902.

[25] V.S. Patankar, Numerical Heat Transfer and Fluid Flow, Hemisphere, New York, 1980.

[26] A.C. Baytas, Buoyancy-driven flow in an enclosure containing time periodic internal sources, Heat and Mass Transfer 31 (1996) 113–119.

[27] A.C. Baytas, Transient natural convection and orientation optimisation in a differentially heated inclined square enclosure with internal heat sources, in: J. Padet, F. Arinc (Eds.), ICHMT, International Symposium on Transient Convective Heat Transfer, Aug. 19–23 (1996), Cesme, Turkey, Begel House, New York, 1997, pp. 117–125.